Very-high-temperature molecular dynamics

Flavien Lambert, Jean Clérouin, and Gilles Zérah
Département de Physique Théorique et Appliquée, CEA/DAM Île-de-France, BP12, 91680 Bruyères-le-Châtel Cedex, France
(Received 25 July 2005; published 19 January 2006)

It is shown that a modified scheme of density functional theory, using the Thomas-Fermi kinetic energy functional for the electrons, is well suited to perform very-high-temperature molecular dynamics simulations on high-Z elements. As an example, iron on the principal Hugoniot is simulated up to 5 keV and 5 times the normal density, giving an equation of state in agreement with current models. Ionic structure is obtained and is given to an excellent level of precision by the structure of the one-component plasma computed for a coupling parameter corresponding to Thomas-Fermi ionization.

DOI: 10.1103/PhysRevE.73.016403 PACS number(s): 52.25.Kn, 02.70.Ns, 71.15.Pd, 71.10.−w

I. INTRODUCTION

Classical molecular dynamics simulations, based on *ad hoc* pair potentials, are limited in temperature and pressure by the repulsive part of the interaction. This pair potential is representative of a given thermodynamic state and cannot be easily transferred to very different situations. As an example, when temperature and density increase, ionization of the atoms strongly modify the strength of the interactions, calling for some sort of self-adjusting potential.

The advantage of *ab initio* calculations rests on the possibility of computing dynamics without requiring any assumptions about the potential between atoms. Indeed, this one is a consequence of Coulomb interactions screened by the electron cloud. Both electrons and ions are taken into account consistently, electrons by minimizing the free energy as a functional of the one-body density in the ions potential [density functional theory (DFT) calculations], and ions are moved under the influence of Coulomb interactions arising from both ions and electrons.

Such quantum molecular dynamics (QMD) simulations have been successfully tested on compressed silica up to 80 000 K and densities twice the normal density [1]. Similarly, QMD simulations were also used to study expanded metals at low densities and temperatures up to 3 eV [2,3] and compressed molecular systems [4]. Unfortunately, calculations based on quantum states at higher temperatures or densities are almost impossible to deal with for two reasons. First, the number of quantum states involved increases strongly with temperature since they are populated according the selected temperature Fermi-Dirac distribution. The difficulty arises from the fact that those bands must be orthogonalized, requiring computer time which scales as the cube of the number of bands. Second, *ab initio* codes are based on pseudopotentials in which a clear separation between core and valence electrons is assumed. Nevertheless, this distinction disappears at high pressure, all electrons being candidates to delocalization sooner or later.

A method was recently proposed by Surh *et al.* [5] to overcome this difficulty by introducing core states in the pseudopotential to treat ionization at high temperature. Interesting results were obtained for aluminum up to 3×10^6 K but no further results have been published for more complex elements. It is clear, nevertheless, that a correct treatment of the electron-ion interaction is the key for describing high-temperature systems.

In this paper, we propose to use an alternative method to a full-orbital QMD calculation. The electronic kinetic and entropic parts of the free energy are expressed implicitly in terms of the density through the Thomas-Fermi functional and combined with a molecular dynamics for ions [Thomas-Fermi molecular dynamics (TFMD) [6,7]]. This approach is consistent with all models of equation of state dealing with hot dense matter such as SESAME [8] or QEOS [9] in which Thomas-Fermi or Thomas-Fermi-Dirac theories are the key ingredients for dealing with the dominant electronic contribution. The method was successfully tested on an hydrogen plasma in conditions close to the center of Jupiter [10,11] and opened a new class of orbital-free methods used in many fields [12].

Well-known difficulties of Thomas-Fermi theory with bound states restrict the method to the plasma regime, and the MD scheme is itself more efficient with strongly coupled plasmas, characterized by a coupling parameter

$$\Gamma = \frac{Z^{*2}e^2}{r_{ws}k_BT}, \tag{1}$$

where $r_{ws}=(3/4\pi n)^{1/3}$ is the ionic mean radius, n the material density, and T the temperature. The charge Z^*, which depends on the thermodynamic conditions, can be determined by the mean ionization degree of the ion, although no unique definition exists for this concept.

When $\Gamma \geqslant 1$ the plasma is strongly coupled and MD is efficient. For example, hydrogen under extreme conditions is quickly fully ionized and a further increase of the temperature reduces the coupling parameter. The system becomes more and more kinetic, making MD useless. On the contrary, for a high-Z element, the increase of the temperature leads to a growth in the ionization, allowing for strong-coupling situations for which MD is particularly well suited.

To emphasize this trend, we have computed pressure and structural properties of iron for thermodynamical conditions corresponding to the principal Hugoniot.

II. THEORETICAL PRELIMINARIES

A. Molecular dynamics

The simultaneous evolution of the electronic density and the ions is realized thanks to a Car-Parrinello- [13] like scheme based on a Lagrangian formulation (atomic units are used throughout the paper)

$$L = \frac{1}{2}\sum_{i=1}^{N_{\text{ions}}} M_i \dot{R}_i^2 - \frac{1}{2}\sum_{i=1}^{N_{\text{ions}}}\sum_{j>i}\frac{Z_i Z_j}{|\mathbf{R}_i - \mathbf{R}_j|} + \frac{1}{2}\mu\int \dot{\rho}^2(\mathbf{r})d\mathbf{r} - F_0[\rho(\mathbf{r}), R_i] + \Lambda\left[\int \rho(\mathbf{r})d\mathbf{r} - N_{\text{electrons}}\right], \tag{2}$$

where ρ and R_i are the dynamical variables associated, respectively, with the electronic density and ionic positions. The last contribution is a Lagrange multiplier which ensures the global neutrality of the system. The Thomas-Fermi free-energy functional $F_0[\rho(\mathbf{r}), R_i]$ can be written

$$F_0[\rho, R_i] = \frac{1}{\beta}\int d\mathbf{r}\left(\rho(\mathbf{r})\Phi(\mathbf{r}) - \frac{2\sqrt{2}}{3\pi^2\beta^{3/2}} I_{3/2}(\Phi(\mathbf{r}))\right) + \int d\mathbf{r}\,\phi(\mathbf{r}, R_i)\rho(\mathbf{r}) + \frac{1}{2}\int d\mathbf{r}d\mathbf{r}'\frac{\rho(\mathbf{r})\rho(\mathbf{r}')}{|\mathbf{r}-\mathbf{r}'|}, \tag{3}$$

where $\phi(\mathbf{r}, R_i)$ is the total ionic potential, I_ν is the Fermi integral of order ν, and

$$\rho(\mathbf{r}) = \frac{2\sqrt{2}}{\pi^2\beta^{3/2}} I_{1/2}(\Phi(\mathbf{r})). \tag{4}$$

From the proper derivatives versus density and ionic coordinates the equations of motion are deduced and the two species are propagated [7].

It is important to recall here that ions and electrons are treated consistently, propagated under their reciprocal influence. This approach is consequently different from [9] and [8], which take into account ions and electrons separately, the first by a given model of equations of state, such that the Cowan's fluid model, and the second by a Thomas-Fermi cell model.

B. Electron-ion interaction

If the Hartree term and the ion-ion term are not difficult to compute, the electron-ion interaction is a source of difficulty due to the divergence of the electrostatic potential and the resulting Thomas-Fermi density near the nucleus. This divergence can be handled in a cell model (CM) by a logarithmic grid, for example [14]. However, such a method is not introduced in an N-body-type resolution where the grid is fixed and cannot be locally adapted to strong gradients. Consequently, a regularization of the bare ionic potential must be adopted and be used as the ion-electron interaction in Eq. (3).

The simplest way consists in smearing out the ions (SI) inside a given cutoff volume, leading to an ion-electron interaction of the form

$$\phi_{SI}(r) = \begin{cases} -\dfrac{Z}{2r_c}\left[3 - \left(\dfrac{r}{r_c}\right)^2\right], & r < r_c \\ -\dfrac{Z}{r}, & r > r_c. \end{cases} \tag{5}$$

This procedure leads to finite, smooth potentials and electronic densities but does not preserve the charge inside the cutoff volume, resulting in overestimated pressures as was mentioned in a previous paper [7].

In order to preserve the electronic density beyond the cutoff radius, and hence the pressure,[1] we introduced a norm-conserving (NC) regularization[2] by imposing an analytical form to the electronic density inside the cutoff volume, as in the procedure developed by Troullier and Martins [15]:

$$\tilde{\rho}(r) = \begin{cases} \dfrac{1}{4\pi}\exp(a + br^2 + cr^4), & r < r_c \\ \rho(r), & r > r_c, \end{cases} \tag{6}$$

where the coefficients a, b, and c are determined by the continuity and electronic density conservation conditions

$$\lim_{r\to r_c}\tilde{\rho}(r) = \rho(r_c), \tag{7}$$

$$\lim_{r\to r_c}\frac{\partial\tilde{\rho}}{\partial r}\bigg|_r = \frac{\partial\rho}{\partial r}\bigg|_{r_c}, \tag{8}$$

$$\int dr r^2\tilde{\rho}(r) = \int dr r^2\rho(r). \tag{9}$$

Once $\tilde{n}$ is determined, the screened potential ϕ_{sc} is computed from the Thomas-Fermi equation in the cell model:

$$\phi_{sc}(r) = \mu - \frac{1}{\beta}I_{1/2}^{-1}\left(\frac{\pi^2\beta^{3/2}}{\sqrt{2}}\tilde{\rho}(r)\right), \tag{10}$$

where μ is the chemical potential.[3]

Finally, the total regularization, shown in Fig. 1, is obtained by subtracting the Hartree's term:

$$\tilde{\phi}(r) = \phi_{sc}(r) - \int d\mathbf{r}'\frac{\tilde{\rho}(\mathbf{r}')}{|\mathbf{r}-\mathbf{r}'|}. \tag{11}$$

The choice of the cutoff radius does not depend on the conservation of pressure since pressure is entirely determined by the electronic density at the edge of the box. Nevertheless, there has to be a compromise between transferability (small cutoff radius) and efficiency in terms of the fast-Fourier-transform (FFT) grid points (large cutoff radius). Care about dynamical properties must also be taken when large cutoff radii are computed. In particular, the absence of

[1] In Thomas-Fermi cell model, the pressure is entirely determined by the electronic density at the edge of the box.

[2] The computation of the regularization is based on the cell model code [14], and the following spherically symmetric quantities are those computed with this code.

[3] Since μ can be determined by the electronic density at the edge of the box, it is the same as $\tilde{\mu}$ derived with the regularized potential.

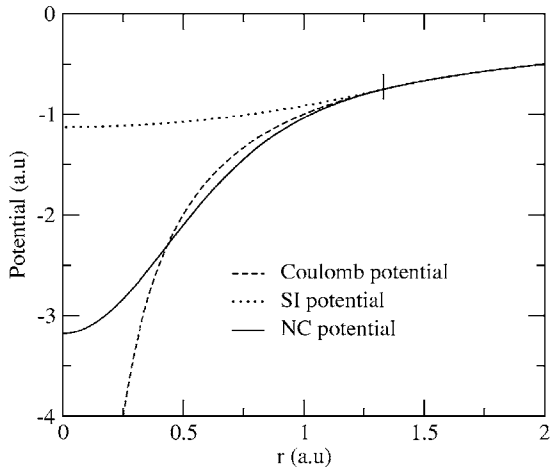

FIG. 1. Bare Coulomb potential compared with the SI potential given by Eq. (5) and with the NC potential given by Eq. (11) with the same cutoff $r_c=1.33$ atomic units for $Z=1$.

interference between cutoff effects (modification of the electronic density) and ion closest approach distance must be checked.

To a certain extent, our procedure is in a spirit of local pseudopotentials developed for orbital-free DFT and applied to solid state [16].

Finally, we would like to emphasize here that the production of the regularization is intrinsically linked to the two theorems of Hohenberg and Kohn [17]. Indeed, ϕ is determined by the variational principle

$$\phi(\mathbf{r}) + \int d\mathbf{r}' \frac{\rho(\mathbf{r}')}{|\mathbf{r}-\mathbf{r}'|} + \frac{\delta \mathcal{F}_K}{\delta \rho(\mathbf{r})} - \mu = 0. \tag{12}$$

The key point is that ϕ in Eq. (12) is the real variable and that ρ is chosen to be $\tilde{\rho}$. Therefore, it has to be noted that the method can be extended to more elaborated functionals.

C. Pressure computation

As previously mentioned, the pressures computed in the CM by the bare Coulomb potential or regularized potential are the same since the electronic density is conserved at the edge of the box. This last statement can be generalized by recalling that this comes from the virial theorem applied to the Thomas-Fermi CM. Therefore, our procedure allows us to reproduce correctly the pressure of the Coulomb potential by using the virial theorem. This one can be written in terms of Fourier transform as [18]

$$3PV = 2K + U_{ee} + U_{ii} + U_{ie} - \int_{|\mathbf{k}|\neq 0} d\mathbf{k} n(\mathbf{k}) S(\mathbf{k}) k \frac{\partial \phi(k)}{\partial k}, \tag{13}$$

where $S(k)$ is the ionic static structure factor, a natural output of the molecular dynamics scheme, the last term taking into account the non-r^{-1} behavior of our potential.

Let us recall that it is necessary to compute a new regularized potential for each thermodynamic conditions in order to get the right "electronic" pressure.

TABLE I. Comparison of the pressures (in Mbar) between the CM and TFMD for iron at 22 g cm^{-3} and $T=50$ eV, versus cutoff and the effect of the number of particles for a given cutoff of $0.9r_{ws}$ for a given grid 32^3 or 64^3.

r_c	P_{CM}	P_{TFMD}	Grid	N	P_{TFMD}
0.3	172.9	175.1	32^3	16	173.5
0.5		176.4		54	173.2
0.7		176.1		128	173.3
0.8		175.9	64^3	16	173.5
				54	173.5
				128	173.5

III. NUMERICAL RESULTS

A. Check of the regularization

As an example, we test the regularization on iron at $T=50$ eV and 22 g cm^{-3} by comparing our results P_{TFMD} with those produced by the cell model P_{CM} [14]. The comparison is indicated in Table I. Both the cutoff radius and FFT grids are involved in order to check the adequacy between the grid and the potential well, determined by the cutoff. The influence of the number of ions has been checked too, since the plane-wave-based code brings into play the ionic structure (bcc in our test).

We emphasize that such an CM resolution uses a very dense radial logarithmic grid (500 grid points) in comparison with the coarse grid used for the three-dimensional (3D) resolution (a 32^3 grid, equivalent to a 16-point radial grid).

Table I shows that a large cutoff radius can be used to minimize the size of the grid. We have also tested that for a given grid (32^3 or 64^3), we can handle 16, 54, or 128 ions without losing precision.

B. QMD simulations

At low temperature, we performed QMD simulations using the VASP *ab initio* simulation package developed at the University of Vienna [19], which couples DFT for the rapidly evolving electron population, with a classical molecular dynamics for the ions. The electron-ion interactions are treated with the projector augmented-wave (PAW) pseudopotentials [20] including eight electrons in the valence. The calculations were performed in the local density approximation (LDA) of DFT as parametrized by Ceperley and Alder [21]. A number of 16 ions was used for MD simulations of iron in thermodynamic conditions along the principal Hugoniot as described in Table II. Following the increase of the temperature, the total number of bands was varied from 100 at 0.1 eV to 400 at 5 eV. Simulations at 10 eV were almost impossible to run with sufficient accuracy. After 500 steps of 1 fs of thermalization, production runs were realized for 1000 steps, allowing the computation of pressures, energies, and structure.

C. TFMD simulations

We turn now to MD simulations of iron over a large range of temperatures and densities along the principal Hugoniot as

TABLE II. Thermodynamic points along the principal Hugoniot of iron, as given by the SESAME EOS No. 2140 (P_S), QMD (P_Q), and TFMD (P_T)

T (eV)	ρ (g cm^{-3})	r_{ws}	Z^*	Γ	θ	P_S (Mbar)	P_Q (Mbar)	P_T (Mbar)
0.1	10	2.46	4.6	800	10^{-3}	0.625	0.467	
1	13.26	2.24	5.3	338	1.1×10^{-2}	3.568	3.517	15.5
5	18.71	1.99	6.1	100	4.5×10^{-2}	15.28	14.91	40
10	22.5	1.88	6.6	62.5	7.9×10^{-2}	33.08		70.3
100	34.5	1.63	10	16.6	0.597	659.9		740
1000	39.65	1.59	20.5	7.4	5.71	14965		14790
5000	34.37	1.63	25.1	2.1	29.9	78573		77564

given in Table II. The average charge state Z^* is obtained by the CM code from the electronic density at the edge of the box, $Z^* = 4/3\,\pi r_{ws}^3 \rho(r_{ws})$. The effective coupling parameter Γ is computed from the precedent value of the charge. The simulations were performed with 54 ions on a grid of 32^3 with a cutoff radius of 0.7 r_{ws} or 0.9 r_{ws}. In order to maintain ionic temperature, ion dynamics calculations were done in the isokinetic ensemble [22] at the electronic temperature. After a first minimization of the electronic free energy, ion dynamics simulations were launched with a set of preconditioned mass ratios μ/M in order to preserve the separation between electronic and ionic frequencies and hence the adiabaticity of the simulation [12].

In order to obtain good statistics on pressure and structural properties, computations were run over several plasma periods, relaxation to equilibrium occurring before two periods. Table II summarizes the results on pressure from SESAME equation of state (EOS) No. 2140, QMD, and TFMD (see also Fig. 2).

We found that QMD pressures are in excellent agreement with the SESAME EOS, except for the lowest temperature, QMD leading to lower pressures than the SESAME one.

As the temperature increases, TFMD results tend to become closer to the SESAME EOS, behavior that was expected. At 100 eV, the discrepancy between SESAME and our results comes from the exchange part of the free energy and the cold curve correction which are introduced in the Thomas-Fermi-Dirac model, which is the basis of the SESAME EOS. The decrease of pressure induced by the exchange part has been widely emphasized by several authors [23]. At lower temperatures, more subtle quantum effects than Pauli exclusion principle play a major role so that Thomas-Fermi model leads to a hugely overestimated pressure when compared to QMD results which treats electrons quantum mechanically. In that case, exchange part, added to 3, would improve the results but give a still too high pressure [23]. In addition to thermodynamical properties, molecular dynamics allowed us to get structural properties, in a consistent description between ions and electrons. The ion-ion pair distribution functions are plotted on the Fig. 3 and compared with those of the one-component plasma (OCP) with a coupling constant computed from Z^*. At highest temperatures,

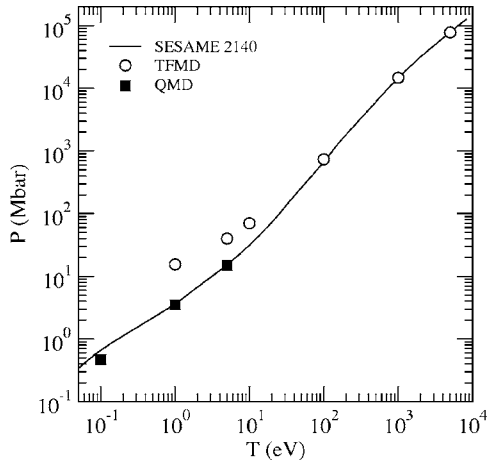

FIG. 2. Principal Hugoniot of iron. Line is SESAME EOS, circles are TFMD results, and squares come from QMD.

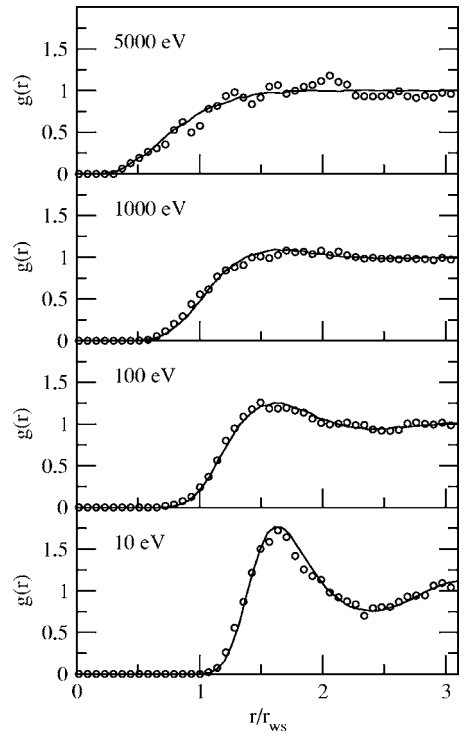

FIG. 3. Ion-ion pair distribution functions. Circles represent our results, and the line is the OCP one computed with the effective Γ^*.

we obtained an interesting match between the two pair distribution functions. Although, the pair distribution function is not a very sensitive quantity to the details of interactions, several quantities like the closest approach distance or the position of the maximum are a good check for comparison. To explain this, we want first to recall that one-component plasma is a theoretical model where classical particles are moving under mutual Coulomb forces, these particles being immersed in a *nonpolarizable* neutralizing background. The key point in the calculation of the "ion charge" is that it involves the electronic density at the edge box $\rho(r_{ws})$ which corresponds to free electrons since electric field vanishes at r_{ws}. Furthermore, Z^* represents the number of free electrons in the CM since

$$\int_{\mathbf{E=0}} d\mathbf{r}\rho(\mathbf{r}) = \rho(r_{ws}) \int d\mathbf{r} = \rho(r_{ws})\frac{4}{3}\pi r_{ws}^3. \qquad (14)$$

Therefore, in view of the pair distribution function, our systems are equivalent to particles composed of an ion with its polarizable electron cloud moving in the nonpolarizable neutralizing background of free electrons.

It is interesting to link this result to the adiabatic approximation which is the basis of our molecular dynamics. Indeed, it can be easily seen in Eq. (2) that the adiabatic approximation transforms the many-body problem involving ions and electrons into two many-body problems, the first in which only the electrons are propagated in a fixed ionic configuration and the second which involved only the ions moving under a screened pair potential. Consequently, our results show that the screened two-body potential is simply a Coulomb potential with the Thomas-Fermi charge.

IV. CONCLUSION

We have shown that the TFMD model is able to compute pressure and structural properties of high-Z elements over a wide range of temperatures along the principal Hugoniot. MD simulations are possible up to a temperature of 5 keV, where interactions still play a major role. We found that if pressures are strongly overestimated at low temperatures when compared with QMD simulations, they fall in reasonable agreement with SESAME tables for temperatures greater than 10 eV, when QMD simulations are no longer possible. An interesting result is that the pair distribution function $g(r)$ is precisely matched by the OCP one computed for an effective coupling parameter given by the Thomas-Fermi ionization. This simple rule could lead to considerable improvements for computing transport properties of such high-temperature plasmas.

[1] Y. Laudernet, J. Clérouin, and S. Mazevet, Phys. Rev. B **70**, 165108 (2004).
[2] M. P. Desjarlais, J. D. Kress, and L. A. Collins, Phys. Rev. E **66**, 025401(R) (2002).
[3] J. Clérouin, P. Renaudin, Y. Laudernet, P. Noiret, and M. P. Desjarlais, Phys. Rev. B **71**, 064203 (2005).
[4] J. D. Kress, S. Mazevet, L. A. Collins, and W. W. Wood, Phys. Rev. B **63**, 024203 (2001).
[5] M. P. Surh, T. W. Barbee III, and L. H. Yang, Phys. Rev. Lett. **86**, 5958 (2001).
[6] G. Zérah, J. Clérouin, and E. L. Pollock, Phys. Rev. Lett. **69**, 446 (1992).
[7] J. Clerouin, E. L. Pollock, and G. Zerah, Phys. Rev. A **46**, 5130 (1992).
[8] SESAME: The Los Alamos National Laboratory Equation of State Database, Report No. LA-UR-92-3407, edited by S. P. Lyon and J. D. Johnson (Group T-1, 1992).
[9] R. M. More, K. H. Warren, D. A. Young, and G. B. Zimmerman, Phys. Fluids **31**, 3059 (1988).
[10] J. I. Penman, J. G. Clérouin, and P. G. Zérah, Phys. Rev. E **51**, R5224 (1995).
[11] J. G. Clérouin and S. Bernard, Phys. Rev. E **56**, 3534 (1997).
[12] M. Pearson, E. Smargiassi, and P. A. Madden, J. Phys.: Condens. Matter **5**, 3221 (1993).
[13] R. Car and M. Parrinello, Phys. Rev. Lett. **55**, 2471 (1985).
[14] W. R. Johnson, FORTRAN program for temperature-dependent Thomas-Fermi atom, http://www.nd.edu/johnson/ (2002).
[15] N. Troullier and J. L. Martins, Phys. Rev. B **43**, 1993 (1991).
[16] S. Watson, B. J. Jesson, E. A. Carter, and P. A. Madden, Europhys. Lett. **41**, 37 (1998).
[17] P. Hohenberg and W. Kohn, Phys. Rev. **136**, B864 (1964).
[18] O. H. Nielsen and R. M. Martin, Phys. Rev. B **32**, 3792 (1985).
[19] G. Kresse and J. Hafner, Phys. Rev. B **47**, R558 (1993).
[20] G. Kresse and D. Joubert, Phys. Rev. B **59**, 1758 (1999).
[21] D. M. Ceperley and B. J. Alder, Phys. Rev. Lett. **45**, 566 (1980).
[22] P. Minary, G. Martyna, and M. Tuckerman, J. Chem. Phys. **118**, 2510 (2003).
[23] P. Fromy, C. Deutsch, and G. Maynard, Phys. Plasmas **3**, 714 (1996).